ISSN 1674-1056
http://cpb.iphy.ac.cn
http://iopscience.iop.org/cpb
中国物理 B
Chinese Physics
中国物理 Chinese Physics B

Novel graphene enhancement nanolaser based on hybrid plasmonic waveguides at optical communication wavelength

Zhengjie Xu(徐政杰), Jun Zhu(朱君), Wenju Xu(徐汶菊), Fu Deli(傅得立), Cong Hu(胡聪), Frank Jiang

Citation: Chin. Phys. B . 2018, 27(8): 088104. **doi:** 10.1088/1674-1056/27/8/088104

Journal homepage: http://cpb.iphy.ac.cn; http://iopscience.iop.org/cpb

What follows is a list of articles you may be interested in

Modulated thermal transport for flexural and in-plane phonons in double-stub graphene nanoribbons

Chang-Ning Pan(潘长宁), Meng-Qiu Long(龙孟秋), Jun He(何军)

Chin. Phys. B . 2018, 27(8): 088101. **doi:** 10.1088/1674-1056/27/8/088101

Free-standing, curled and partially reduced graphene oxide network as sulfur host for high-performance lithium-sulfur batteries

Hui-Liang Chen(陈辉亮), Zhuo-Jian Xiao(肖卓建), Nan Zhang(张楠), Shi-Qi Xiao(肖仕奇), Xiao-Gang Xia(夏晓刚), Wei Xi(席薇), Yan-Chun Wang(王艳春), Wei-Ya Zhou(周维亚), Si-Shen Xie(解思深)

Chin. Phys. B . 2018, 27(6): 068101. **doi:** 10.1088/1674-1056/27/6/068101

Facilitative effect of graphene quantum dots in MoS_2 growth process by chemical vapor deposition

Lu Zhang(张璐), Yongsheng Wang(王永生), Yanfang Dong(董艳芳), Xuan Zhao(赵宣), Chen Fu(付晨), Dawei He(何大伟)

Chin. Phys. B . 2018, 27(1): 018101. **doi:** 10.1088/1674-1056/27/1/018101

Photoconductive multi-layer graphene photodetectors fabricated on etched silicon-on-insulator substrates

Yu-Bing Wang(王玉冰), Wei-Hong Yin(尹伟红), Qin Han(韩勤), Xiao-Hong Yang(杨晓红), Han Ye(叶焓), Qian-Qian Lv(吕倩倩), Dong-Dong Yin(尹冬冬)

Chin. Phys. B . 2017, 26(2): 028101. **doi:** 10.1088/1674-1056/26/2/028101

Low specific contact resistivity to graphene achieved by AuGe/Ni/Au and annealing process

Shu-Zhen Yu(于淑珍), Yan Song(宋焱), Jian-Rong Dong(董建荣), Yu-Run Sun(孙玉润), Yong-Ming Zhao(赵勇明), Yang He(何洋)

Chin. Phys. B . 2016, 25(11): 118101. **doi:** 10.1088/1674-1056/25/11/118101

SPECIAL TOPIC — Nanophotonics

Novel graphene enhancement nanolaser based on hybrid plasmonic waveguides at optical communication wavelength*

Zhengjie Xu(徐政杰)[1], Jun Zhu(朱君)[1,2,†], Wenju Xu(徐汶菊)[1], Deli Fu(傅得立)[1], Cong Hu(胡聪)[2], and Frank Jiang[1,‡]

[1] College of Electronic Engineering, Guangxi Normal University, Guilin 541004, China
[2] Guangxi Key Laboratory of Automatic Detecting Technology and Instruments, Guilin University of Electronic Technology, Guilin 541004, China

(Received 7 December 2017; revised manuscript received 2 January 2018; published online 25 July 2018)

Surface plasmon polariton (SPP) nanolaser, which can achieve an all-optical circuit, is a major research topic in the field of micro light source. In this study, we examine a novel SPP graphene nanolaser in an optoelectronic integration field. The proposed nanolaser consists of metallic silver, two-dimensional (2D) graphene and high refractive index semiconductor of indium gallium arsenide phosphorus. Compared with other metals, Ag can reduce the threshold and propagation loss. The SPP field, excited by coupling Ag and InGaAsP, can be enhanced by the 2D material of graphene. In the proposed nanolaser, the maximum value of propagation loss is approximately 0.055 dB/μm, and the normalized mode area is constantly less than 0.05, and the best threshold can achieve 3380 cm^{-1} simultaneously. Meanwhile, the proposed nanolaser can be fabricated by conventional materials and work in optical communication (1550 nm), which can be easily achieved with current nanotechnology. It is also an important method that will be used to overcome the challenges of high speed, miniaturization, and integration in optoelectronic integrated technology.

Keywords: graphene, SPP nanolaser, optical communication

PACS: 81.15.Gh, 81.40.Lm **DOI:** 10.1088/1674-1056/27/8/088104

1. Introduction

Surface plasmon polariton (SPP) is an electromagnetic mode of optical wave and transferable surface charge, and it changes the sub-wavelength structure of surface metal. These electromagnetic waves travel along the metal–dielectric or metal–air interface and originate from the interaction between light and collective electron oscillation on metal surface.[1–3] Mark *et al.* proposed an SPP nanolaser based on theoretical prediction.[4] This nanolaser was experimentally demonstrated by Norginov.[5] Oulton proposed a typical hybrid plasmonic waveguide structure composed of a high-index dielectric nanowire above a flat metal substrate separated by a low-index buffer layer, which exhibits low loss and confined nanoscale field.[6] Bian[7,8] proposed several new hybrid plasmonic structures, including a coupled nanowire pair based plasmonic laser structure and a coplanar edge-coupled plasmonic waveguide structure, which can be used for subwavelength-scale nanolaser with low threshold. Guillaume[9] proposed a nanolaser based on hybrid indium phosphide-on-silicon. A hybrid plasmonic waveguide consisting of InGaAsP semiconductor on the top of an Ag substrate separated by an Si buffer layer was investigated in Ref. [10]. However, the waveguide presents complex structure and spread energy, thereby restricting the optoelectronic integration; the propagation distance is also too short to achieve highly integrated photo-communication.

Then, with the rapidly development of nanophotonics, an increasingly number of two-dimensional (2D) materials were used to improve the performance in waveguide, such as Bi_2Se3,[11] WS2,[12] graphene and hBN.[13] Recently, by using the ion beam modified graphene/WSe2 heterostructure as a saturable absorber, Q-switched pulsed lasing with optimized performance has been realized in yttrium aluminum garnet ceramic waveguide cavity.[14] The aforementioned studies indicated the outstanding performance of combing two dimensional materials with conventional waveguides. We further study the interaction between graphene and the SPP nanolaser based on the current research status.

In this paper, we design a graphene enhancement nanolaser based on hybrid plasmonic waveguides at optical communication wavelength. Firstly, the finite-element method is used to analyze the electric field distribution and calculate the modal characteristics in the optical communication wavelength at 1550 nm. Furthermore, in order to obtain the optimal mode parameters and threshold, structural properties of

*Project supported by the Guangxi Natural Science Foundation, China (Grant No. 2017GXNSFAA198261), the National Natural Science Foundation of China (Grant No. 61762018), the Guangxi Youth Talent Program, China (Grant No. F-KA16016), the Guangxi Normal University Key Program, China (Grant No. 2015ZD03), the Innovation Project of Guangxi Graduate Education, China (Grant Nos. XYCSZ2018082, XJGY201807, and XJGY201811), and the Guangxi Key Laboratory of Automatic Detecting Technology and Instruments, China (Grant No. YQ16206).

†Corresponding author. E-mail: zhujun1985@gxnu.edu.cn
‡Corresponding author. E-mail: franksydney2008@qq.com

© 2018 Chinese Physical Society and IOP Publishing Ltd

proposed waveguide are calculated. Then, the performance of proposed waveguide is compared with those from other studies; we observe a significant improvement. Finally, we further study the threshold and mode parameters in the cases with and without graphene. We find that the proposed waveguide has significant potential applications in ultrahigh density plasma devices and photonic integrated circuit.

2. Structure and method

The structure of SPP waveguide is schematically illustrated in Fig. 1(a), and the 2D section diagram is depicted in Fig. 1(b).

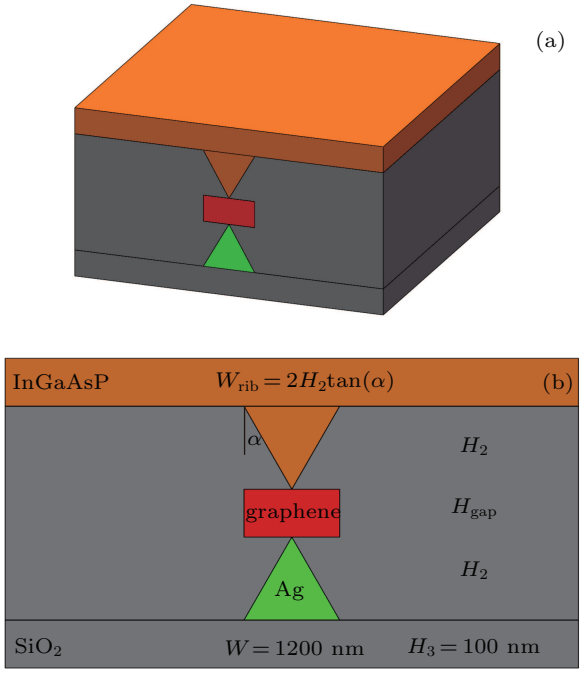


Fig. 1. (color online) (a) Proposed structure of three-dimensional (3D) SPP waveguide. (b) 2D section diagram along *x*–*y*.

The proposed structure consists of SiO_2 substrate, Ag triangular rib, graphene layer, and inverted ridge high refractive index semiconductor of InGaAsP, arranged in the order from the bottom to the top. Sliver is selected because of its low propagation loss in the optical communication range compared with others, and the material of InGaAsP can provide gain compensation, which can further enhance SPP photon localization. Graphene is located in the middle of two tips, which effectively enhances and restricts the SPP. Mode parameters, are important to reflect waveguide performance, including modal effective index ($n_{\rm eff}$), propagation loss ($\alpha_{\rm eff}$), normalized mode area (SF), and confinement factor (Γ).

Modal effective index ($n_{\rm eff}$) is reflected by the real part of the hybrid waveguide propagation constant and the free-space wave vector.

Normalized mode area (SF), which is defined as the ratio of the effective mode area ($A_{\rm m}$) to the diffraction-limited mode area (A_0), can be expressed as $\mathrm{SF} = A_{\rm m}/A_0$.[7] The effective mode area ($A_{\rm m}$) is calculated from the following equation:

$$A_{\rm m} = \frac{[\iint_{A_\infty} |E|^2 \,\mathrm{d}A]^2}{\iint_{A_\infty} |E|^4 \,\mathrm{d}A}, \tag{1}$$

where E is the electric field intensity of the hybrid mode and A_0 is the diffraction-limited mode area and defined as $A_0 = \lambda^2/4$, with λ being the incident wavelength.

Propagation loss ($\alpha_{\rm eff}$) is reflected by the imaginary part of the hybrid waveguide propagation constant and the free-space wave vector, and can be expressed as[7]

$$\alpha_{\rm eff} = 20\lg(e)\, n_{\rm im} k_0 = 10\frac{\lg(e)}{L_{\rm p}}, \tag{2}$$

where e and $L_{\rm p}$ are the Euler's number and propagation distance.

Confinement factor (Γ) refers to the capability of the gain nanowire to confine mode field, and is defined as follows:[8]

$$\Gamma = \frac{W_{\rm s}}{W} = \frac{\iint_s W(r)\,\mathrm{d}A}{\iint_{\rm all} W(r)\,\mathrm{d}A}, \tag{3}$$

where $W_{\rm s}$ is the electric energy in the gain medium, and W is the total electric energy of the mode.

The pump threshold for lasing is related to the end facet reflectivity R which is calculated from the following equation[8]

$$R = (n_{\rm eff} - 1)/(n_{\rm eff} + 1). \tag{4}$$

The lasing threshold can be calculated using the following formula:

$$g_{\rm th} = (k_0\alpha_{\rm eff} + \ln(1/R)/L)/\Gamma(n_{\rm eff}/n_{\rm wire}), \tag{5}$$

where $k_0 = 2\pi/\lambda$, $n_{\rm eff}$ and $n_{\rm wire}$ are the mode effective index and refractive index of the gain nanowire, respectively, $\alpha_{\rm eff}$ is the propagation loss, Γ denotes confinement factor, and L is defined as the length of waveguide, fixed at 30 μm.

Graphene's out-of-plane permittivity is set to be 2.25, and its in-plane permittivity[15] can be expressed as

$$\varepsilon_{\rm g} = -\sigma_{\rm g,i}/\varepsilon_0\omega t + \mathrm{i}\sigma_{\rm g,r}/\varepsilon_0\omega t, \tag{6}$$

where $\sigma_{\rm g,i}$ and $\sigma_{\rm g,r}$ represent the imaginary and real part of the conductivity of graphene $\sigma(\omega)$, and ε_0 and $t = 0.3$ nm denote the vacuum permittivity and thickness of graphene, respectively.

The conductivity of graphene $\sigma(\omega)$ is modeled using the Drude model with D (Drude weight) and Γ (scattering width) used as two fitting parameters:[16,17]

$$\sigma(\omega) = \frac{\mathrm{i}D}{\pi(\omega + \mathrm{i}\Gamma)}, \tag{7}$$

where ω is the incident light frequency, $D = e^2E_{\rm F}/\hbar^2$ and $\Gamma = \tau^{-1} = eV_{\rm F}^2/\mu E_{\rm F}$, with e being the elementary charge, $\hbar$ the reduced Planck's constant, $E_{\rm F}$ the Fermi energy level, μ the carrier mobility, $V_{\rm F} \approx 2.1^{1/2} \times 10^6$ m·s^{-1} the Fermi velocity, and τ the intrinsic relaxation time.

3. Results and discussion

3.1. Electric field distribution

We compare the electric field distribution in the case with graphene and that without graphene in the same circumstance. The novel phenomenon can be found that graphene not only can enhance SPP coupling effect, but also can restrict the electric field.

The height and the length of Ag and InGaAsP triangular structure are denoted as H_2 and $W_{\rm rib}$, respectively (here $W_{\rm rib} = 2H_2 * \tan(\alpha)$). The thickness of rectangle graphene layer is denoted as $H_{\rm gap}$ and the length of SiO_2 basement is represented with W.

In fundamental simulation, the parameters are set to be $H_2 = 120$ nm, $H_{\rm gap} = H_{\rm g} = 0.3$ nm, $W = 800$ nm, $\alpha = \pi/M6$, and $H_3 = 100$ nm. The Fermi energy level and carrier mobility are set to be $E_{\rm F} = 0.8$ eV and $\mu = 1$ m^2/(V·s), respectively. Because we focus on the SPP performance, we analyze the electric field based on the contact point between Ag and graphene for different $H_{\rm gap}$ as shown in Figs. 2(a)–2(f).

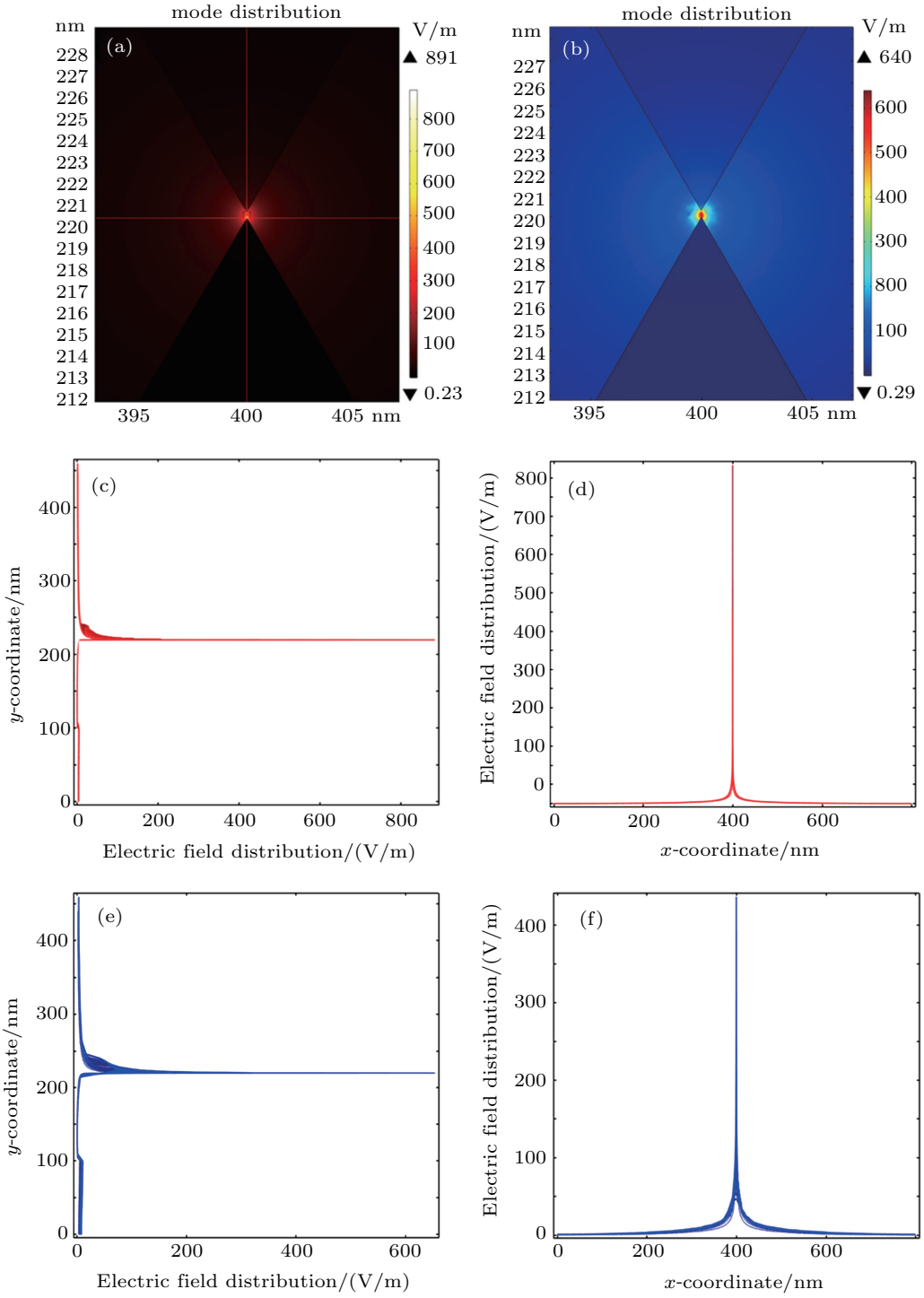


Fig. 2. (color online) Fundamental electric distributions with (a) and without (b) graphene. Field distributions along (c) horizontal and (d) vertical red solid lines in panel (a) with graphene. Field distributions along (e) the horizontal and (f) the vertical direction in panel (b) with no graphene.

Figure 2(a) shows that coupling excitation electric field with graphene can be easily achieved at 891 V/m. However, in Fig. 2(b), the maximum value of electric field strength without graphene is approximately 640 V/m. It shows that the electric field in the graphene significantly increases by nearly 40%, compared with that without graphene. Therefore, we can find that graphene can extremely enhance the electric field strength. A comparison between Figs. 2(c) and 2(e) shows that the electric field distribution with graphene layer, along the vertical red solid line, is more concentrated at $y = 220$ nm in SPP waveguide. As shown in Figs. 2(d) and 2(f), the electric field distribution in the case with no graphene partially diverges in the $x = 400$ nm direction. Just as figures 2(c) and 2(d) indicate the curve of electric filed distribution in the case with graphene is for a divergent state, whereas figures 2(e) and 2(f) present that it is a polymerization state in the case without graphene.

Therefore, we can conclude that the electric field can be excellently confined in the rectanglar graphene layer.

3.2. Mode parameters

We conduct the quantitative analysis of mode parameter by changing thickness of the rectangular graphene layer, H_{gap}. Considering the limitations of the current manufacturing process, the width and length of a rectangular are set to be unequal to increasing its feasibility. The most important parameters in the SPP waveguide are electric field distribution and mode parameters which include modal effective index (n_{eff}), propagation loss (α_{eff}), normalized mode area (SF), and confinement factor (Γ). The mode parameter will be analyzed in the following.

In the calculation, the frequency of incident light is set to be 1550 nm and the structure parameter of H_2, H_{gap}, W are set to be 120 nm, 0.3 nm, and 800 nm, respectively. The 3D normalized electric field strength is shown in Fig. 3.

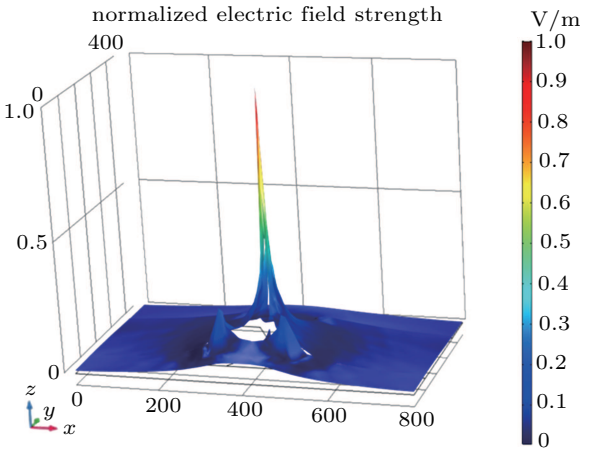


Fig. 3. (color online) Normalized electric field strength.

As shown in Fig. 3, the electric field coupled by Ag and InGaAsP is normalized. After the electric filed strength is normalized, the strong couple effect and peak value appear in the interface between Ag and graphene. Due to the ohmic effect of metal, some energy spreads to the bottom of triangle. Then, SPP effect is excited by Ag and SiO_2, resulting in propagation loss. From the normalized electric field distribution, energy is confined into a small area, which indicates that the proposed structure has an outstanding performance in mode area and confinement factor.

Then, in order to obtain the best structure characteristic, we further study the mode parameter in the waveguide. Considering the completeness of the simulation, we change the thickness of graphene, H_{gap}, from 0.3 nm to 20.3 nm in steps of 0.2 nm for different H_2 as shown in Figs. 4(a)–4(d).

Figures 4(a) and 4(b) show that when the height of triangle (H_2) is fixed, the modal effective index decreases as the thickness of the rectangular graphene (H_{gap}) increases. The reason is that the coupling effect between Ag and InGaAsP weakens as H_{gap} increases, which means that it excites less energy. In addition, when the thickness of graphene (H_{gap}) is fixed, the modal effective index increases as H_2 decreases. Then, we analyze the propagation loss which is defined as the loss of light transmission in the waveguide. Therefore, the lower propagation loss value is expected. When the height of triangle (H_2) is fixed, propagation loss increases as H_{gap} increases. As the Ag triangle area increases, metal produces a greater ohmic effect, moving the energy to the two corners of the triangle. Thus, the larger Ag triangle area produces higher modal effective index and lower propagation loss with maximum values of nearly 3 and 0.055 dB/μm, respectively. Compared with the maximum, 0.1 dB/μm, the propagation loss decreases in the order of magnitude.[7,18] Therefore, the proposed waveguide has outstanding propagation property.

Normalized mode area, which is defined as the optical limit capability in waveguide structure, indicates the degree of energy concentration. The relationships between H_{gap} and normalized mode area for different H_2 are shown in Fig. 4(c). As graphene thickens, more energy diverges into the rectangular range. When H_{gap} is fixed, normalized mode area increases as the H_2 increases. With the decrease of coupling effect, high energy has stronger constraining force than low energy.

The maximum and the minimum value in the proposed waveguide are 0.05 and 0.001, respectively. However, in Ref. [19], the maximum and minimum values are 0.4 and 0.1, respectively. Compared with the maximum 0.1 in Ref. [7] , the normalized mode area is reduced by two orders of magnitude. Thus, the normalized mode area of the proposed waveguide improves about 87.5% (nearly one order of magnitude), showing a strong limit.

The confinement factor is defined as the physical quantity that can reflect the capability of energy distribution in the waveguide. Thus, in this paper, it is defined as the ratio of the energy in the gain medium to the total energy of the mode

field. The relationship among H_2, H_{gap}, and confinement factor are shown in Fig. 4(d). As H_{gap} increases, the coupling effect weakens, resulting in energy divergence and increasing confinement factor.

In the proposed waveguide, the maximum value of confinement factor is 0.8, which is comparable to that in Ref. [19], the maximum value and the minimum value are 0.35 and 0.15, respectively. The performance of our proposed waveguide is improved by more than 56%. Energy is limited around graphene, proving its capability in constrained optical field. Then, we discuss the most important parameter reflecting the optical transmission property. As shown in Figs. 2(a)–2(d), we select waveguide length to be $L = 30$ μm to calculate the threshold. When H_2 is fixed, threshold decreases as H_{gap} increases. It leads the energy to decrease as the coupling effect weakens.

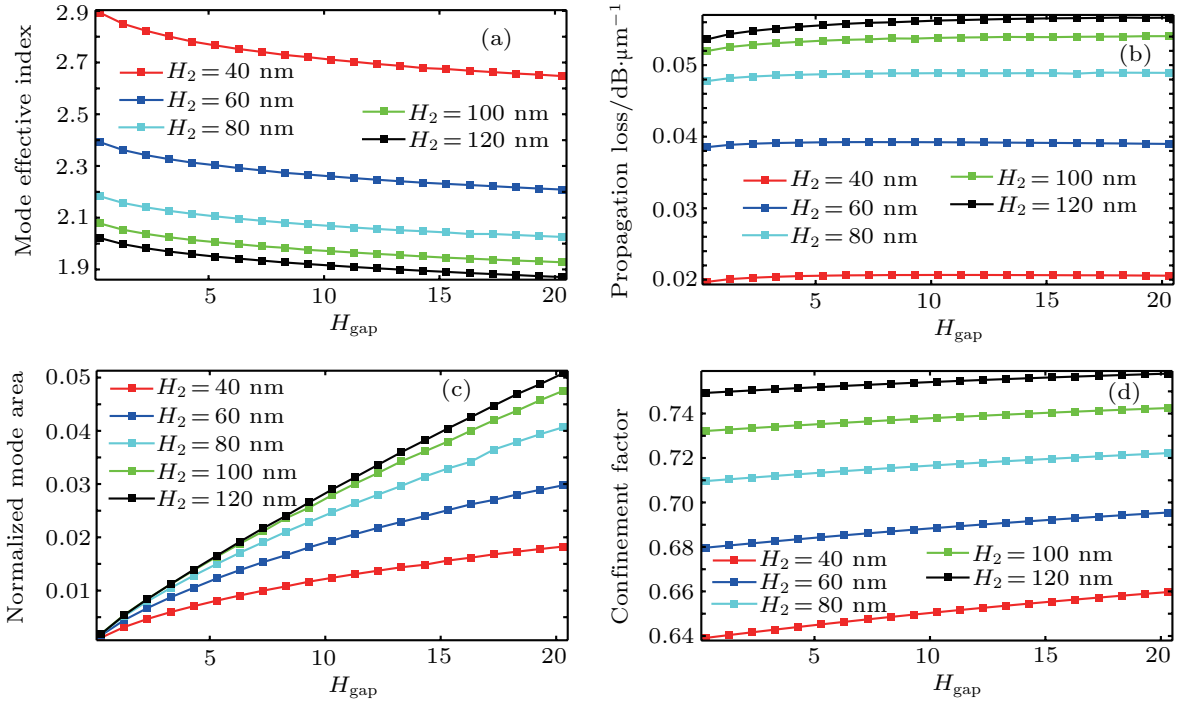


Fig. 4. (color online) Mode parameters appearing in waveguide, showing (a) modal effective index, (b) propagation loss, (c) normalized mode area, and (d) confinement factor.

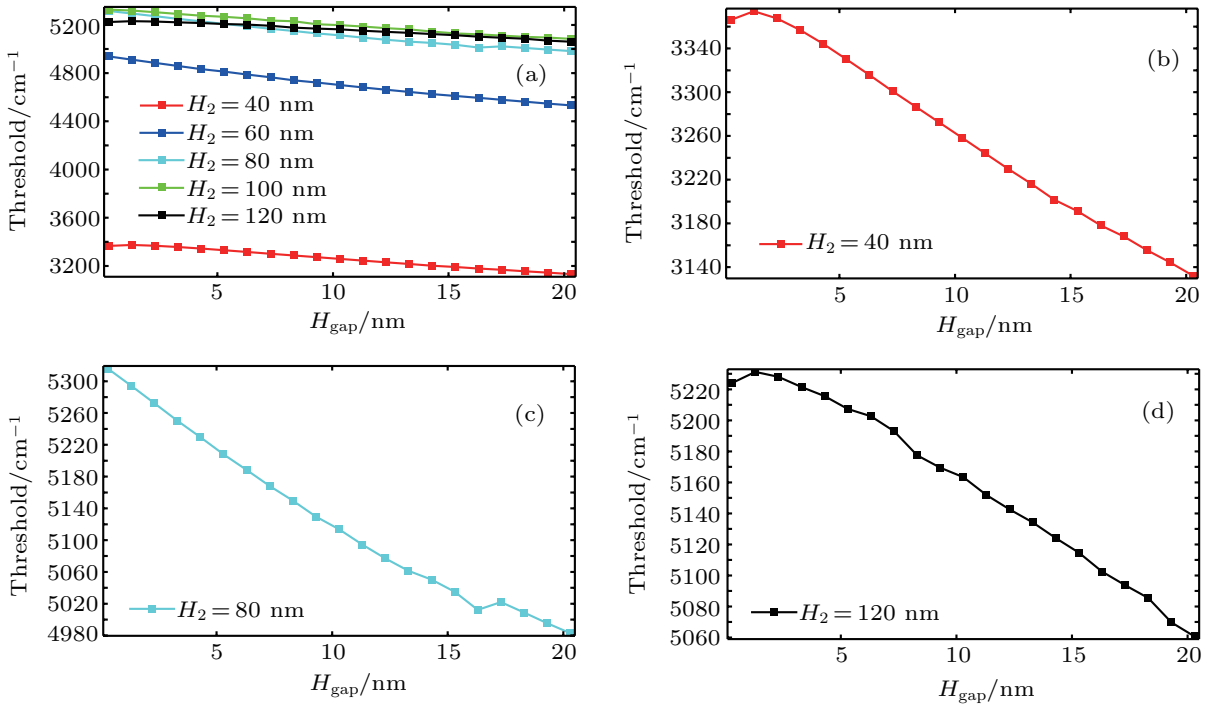


Fig. 5. (color online) Thresholds versus H_{gap} for different H_2 values.

After aforementioned analysis, the best structure parameter can be obtained in the cases of $H_{gap} = 1.3$ nm and $H_2 = 40$ nm. The best threshold, 3380 cm^{-1}, has the same order of magnitude as that in Ref. [18]. However, in the proposed waveguide, the best normalized mode area and mode area are 0.0025 and $10^{-9}\lambda^2$, respectively. The proposed waveguide shows the better confinement factor, normalized mode area, and propagation loss than other structures.

Last but not least, as shown in Table 1, based on the best structure parameter, the mode parameter of the proposed waveguide, including modal effective index (n_{eff}), propagation loss (α_{eff}), normalized mode area (SF), confinement factor (Γ), and threshold, will be further studied in the cases with and without graphene, respectively.

Table 1. Mode parameters for the cases with and without graphene.

	n_{eff}	α_{eff}/(dB/cm)	SF/10^{-3}	Γ	Threshold/cm^{-1}
With graphene	2.851	203	3.1	0.645	3375
Without graphene	2.822	200	1.9	0.360	6060

As shown in Table 1, the mode parameters of proposed waveguide can be obtained in the cases with and without graphene, respectively. Comparing with in the case without graphene, the confinement factor in the case with graphene, which can reflect the capability of energy distribution, shows a better value of 0.645. The threshold of waveguide with and without graphene free are 3375 cm^{-1} and 6060 cm^{-1}, respectively. Therefore, it can indicate that graphene has the ability to concentrate energy and reduce threshold. However, because of the scattering mechanism in graphene, the propagation loss of the proposed waveguide is larger than that in the case without graphene free.

4. Conclusions

According to the aforementioned analysis, we propose a novel graphene enhancement nanolaser based on the hybrid plasmonic waveguide at an optical communication wavelength of 1550 nm. In this paper, we find that the graphene has the properties to limit SPP and enhance coupling effect. Then, based on the best structural property, the optimal confinement factor and propagation loss are 0.645 and 0.02, respectively. The threshold and normalized mode area are 3380 cm^{-1} and 0.0025, respectively. Compared with the waveguide in other studies, our waveguide is improved nearly 56.52% in confinement factor and reduced in propagation loss. Meanwhile, the normalized mode area increases about 87.5%. In addition, the proposed waveguide can be fabricated by using normal materials, which can be achieved easily by current nanotechnology. This method can be used to solve the difficult problems of high-speed, miniaturization and integration in optoelectronic integrated technology in the future.

References

[1] Maier S A 2006 *IEEE J. Sel. Top. Quantum Electron.* **12** 1671
[2] Gramotnev D K and Bozhevolnyi S I 2010 *Nat. Photon.* **4** 83
[3] William L B, Dereux A and Ebbesen T W 2003 *Nature* **424** 824
[4] Bergman D J and Stockman M I 2003 *Phys. Rev. Lett.* **90** 027402
[5] Noginov M A, Zhu G and Belgrave A M 2009 *Nature* **460** 1110
[6] Oulton R F, Sorger V J and Zentgraf T 2009 *Nature* **461** 629
[7] Bian Y S, Zheng Z and Liu Y 2011 *IEEE Photon. Tech. Lett.* **23** 884
[8] Bian Y S, Zheng Z and Zhao X 2013 *Opt. Commun.* **287** 245
[9] Mu J W, Chen L and Li X 2013 *Appl. Phys. Lett.* **103** 131107
[10] Babak O, Habib K and Sirous K 2015 *Opt. Quantum Electron.* **47** 1791
[11] Tan Y, Zhang Han and Zhao C J 2015 *Opt. Lett.* **40** 637
[12] Tan Y, Guo Z N and Ma L N 2016 *Opt. Express* **24** 2858
[13] Chen X, Wang Y and Xiang Y J 2016 *J. Lightwave. Technol.* **34** 4948
[14] Tan Y, Liu X B and He Z L 2017 *ACS Photon.* **4** 1513
[15] Vakil A and Engheta N 2011 *Nature* **332** 1291
[16] Gao W L, Shu J and Qiu C Y 2012 *ACS Nano* **6** 7806
[17] Yan H G, Xia F N and Zhu W J 2011 *ACS Nano* **5** 9854
[18] Li Z Q, Piao R Q and Zhao J J 2015 *J. Opt.* **17** 125008
[19] Bian Y S, Zheng Z and Zhao X 2013 *Opt. Commun.* **287** 245